Revista Brasileira de Geofísica
RBGf
Brazilian Journal of Geophysics

Revista Brasileira de Geofísica (2006) 24(3): 429-439

ISSN 0102-261X
www.scielo.br/rbg

LINEAR INVERSION OF A NEGATIVE GRAVITY ANOMALY IN SE RIO GRANDE CONE: A GRABEN ON OCEANIC CRUST?

Emilson Pereira Leite[1] and Naomi Ussami[2]

Recebido em 19 maio, 2006 / Aceito em 29 setembro, 2006
Received on May 19, 2006 / Accepted on September 29, 2006

ABSTRACT. We detect, for the first time, a negative free-air gravity anomaly of 23 mGal amplitude over a region in the South Atlantic Ocean centered at 48°W and 35°S. To this end, we used the integration of conventional shipborne gravity data and gravity data derived from GEOSAT/ERM satellite altimetry. The north bound of this anomaly coincides with the Chuí Lineament and the south bound indicates another lineament, which is the extension of the Meteor Fracture Zone. The anomaly trend is NE-SW, its width is 400 km and its length is 600 km. Two-dimensional linear inversion with relative and absolute equality constraints was used to calculate the density distribution along three profiles perpendicular to the main axis of the anomaly. The result suggests that the sediment thickness in the deepest part of the basin is at least 3.0 km where the ocean bathymetry is 4,800 m. This tectonic feature, an asymmetric half-graben formed between two lineaments, probably lies over an oceanic crust. The estimated volume of sediments in this basin is approximately 50% of the post-Miocene sediments volume deposited in the Rio Grande Cone where gas-hydrates were found.

Keywords: Potential Methods, Gravity Inversion, Rio Grande Cone, Oceanic Crust.

RESUMO. Uma anomalia ar-livre com amplitude negativa de 23 mGal em uma região no oceano Atlântico Sul, centrada em 48°W e 35°S, foi observada pela primeira vez devido à integração de dados de gravimetria marinha convencionais e dados de gravidade derivados de altimetria por satélite, adquiridos pela missão GEOSAT/ERM. O limite norte desta anomalia coincide com o Lineamento Chuí e o limite sul indica outro lineamento, que é uma extensão da Zona de Fratura Meteoro. A anomalia tem direção NE-SW, sua largura é de 400 km e seu comprimento é de 600 km. Foi utilizada uma metodologia de inversão linear bidimensional, com vínculos relativos e absolutos, para calcular a distribuição de densidades ao longo de três perfis paralelos ao eixo principal da anomalia. O resultado sugere que a espessura de sedimentos na parte mais profunda da bacia é de no mínimo 3,0 km onde a batimetria oceânica é de 4.800 m. Esta feição tectônica, um semi-gráben assimétrico formado entre dois lineamentos, provavelmente situa-se sobre uma crosta oceânica. O volume de sedimentos estimado para esta bacia é de cerca de 50% do volume de sedimentos pós-Mioceno depositados no Rio Grande Cone, onde hidratos de gás foram encontrados.

Palavras-chave: Métodos potenciais, Inversão gravimétrica, Cone do Rio Grande, Crosta oceânica.

[1]Department of Geology and Natural Resources, Institute of Geosciences, State University of Campinas, 13083-970 Campinas, SP, Brazil. Postal box: 6152, Tel: (19) 3521-4697; Fax: (19) 3289-1562 – E-mail: emilson@ige.unicamp.br

[2] Department of Geophysics, Institute of Astronomy, Geophysics and Atmospheric Sciences, University of São Paulo, Rua do Matão, 1226 – 05508-900 São Paulo, SP, Brazil. Tel: (11) 3091-4787; Fax: (11) 3091-5034 – E-mail: naomi@iag.usp.br

INTRODUCTION

A free-air anomaly map in Southern Atlantic was obtained through integration of conventional shipborne gravity data and gravity data derived from GEOSAT/ERM satellite altimetry (Fig. 1), using the Least Squares Collocation technique (Leite et al., 1999). This technique assumes that a set of observations associated to any component of the Earths gravity field can be related to the anomalous gravitational potential through appropriate linear functionals. If the covariances between such components are known, then it is possible to estimate any other component of the Earths gravity field. This allows two or more components to be integrated, so that the output can be any one of them for a given study area. The errors associated with the observations and with the estimated quantities are taken into account rigorously in the Least Squares Collocation. Gravity free-air anomalies and height anomalies are the components of the Earths gravity field that were used in the estimation of the free-air anomalies used in this study.

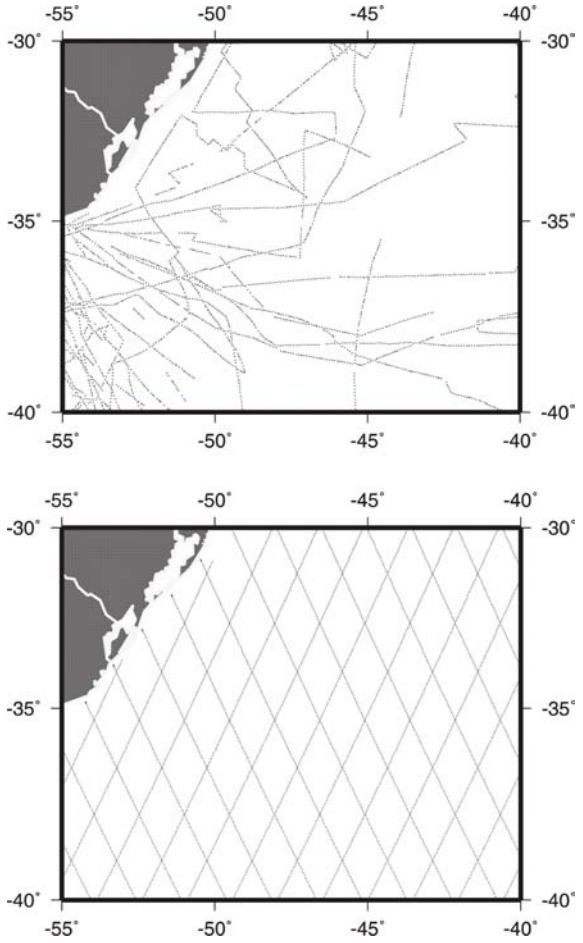

Figure 1 – (a) Conventional shipborne gravity data; (b) satellite altimetry (GEOSAT/ERM).

The free-air anomaly map defined a negative gravity anomaly (Fig. 2) centered at 48°W and 35°S, on the southeast border of Rio Grande Cone (Fontana, 1992). Figure 2 also shows the main physiographic features in the region. To the authors knowledge, this anomaly has never been mapped before because it was used gravity datasets either from the conventional shipborne survey or derived from satellite altimetry (e.g. Andersen & Knudsen, 1995). This paper shows the advantage of using an integrated approach in mapping marine gravity anomalies. Figure 2 also shows the main physiographic features in the region, which are the São Paulo Plateau, the Rio Grande Rise, the Pelotas Basin, the Rio-Grandense Shield and the Rio Grande Cone.

Contrary to interactive forward modeling, an inversion method does not require a complete knowledge about the anomalous source. Rather, an inversion method requires few prior geologic constraints which must be mathematically incorporated by the method in an automatic way. This procedure is frequently adopted to obtain a unique and stable solution in gravity interpretation (Silva et al., 2002).

In this study, we have been working only with constrained linear inversion using the same idea described in Barbosa et al. (1997). The difference here is that we estimated the density contrast distribution that fits the observed anomaly within the measurement errors and represents smooth spatial density variations (Barbosa et al., 2002). So, a discrete density distribution is estimated by standard linear inversion stabilized by imposing smooth spatial density variations. The premise of a smooth spatial density distribution is justified by smooth spatial distributions of gravity values along selected gravity anomaly profiles, i.e. high wavenumber anomalies that could represent real anomalous sources within the crust are not detectable in these profiles.

In this paper, we estimate the discrete density distribution along three gravity profiles over the SE Rio Grande Cone by using an inverse technique which incorporates relative constraints and absolute equality constraints (Barbosa et al., 1997). In the inversions presented here, relative constraints are used to guarantee smooth spatial density variations, while equality constraints are used to set density values associated with specific cells which define the interpretation model.

As most of the geophysical data inversion techniques, the main issue in the proposed methodology is how to set the constraints. If one does not have a set of known density values provided by independent geophysical methods or if the knowledge about the geological setting in the study area is insufficient, this method may not be applied properly or else, the solution may not have any geological meaning.

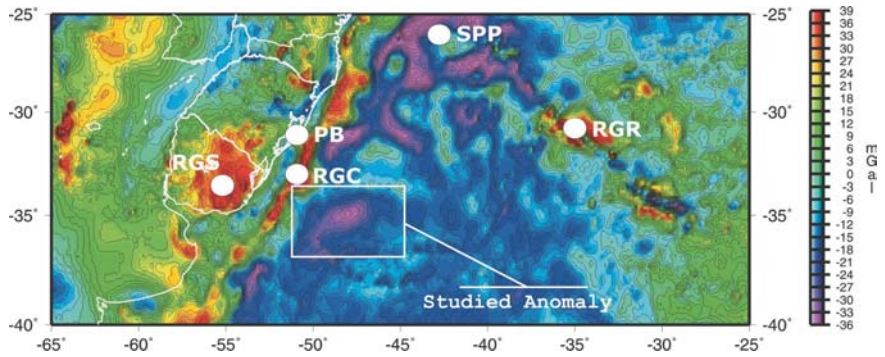

Figure 2 – Main physiographic features over the study region (circles): SPP – São Paulo Plateau; RGR – Rio Grande Rise; PB – Pelotas Basin; RGS – Rio-Grandense Shield; RGC – Rio Grande Cone.

RESIDUAL GRAVITY ANOMALY MODELING

The Earths Gravity Field is produced by a superposition of overlapping gravitational effects of many sources within the crust. Local gravity anomalies associated with near surface masses are referred as to residual anomalies and gravity anomalies due to larger and deeper geological features are referred as to regional anomalies.

In order to obtain the residual anomaly of the region shown in Figure 1, firstly we calculated the gravitational effect due to bending of the crust-mantle interface in response to sedimentary loads in order to check whether this component was important on the observed anomaly.

We also removed from the observed anomaly a polynomial flat surface, which is a regional field that represents sources deeper than about 10 km.

The following sections describe how the residual gravity anomaly was obtained.

Flexural Effect of Sedimentary Loads

Lithosphere and crust-mantle boundary is flexed due to sedimentary loads and this deformation produces long wavelength components on the gravity field. Thus, it is necessary to calculate the gravitational effect of this flexure and to remove it from the observed anomalies.

A sediment isopach map (Emery & Uchupi, 1984) based on reflection and refraction seismic, well stratigraphy, and DSDP (Deep Sea Drilling Project) data were digitized (Fig. 3).

Next to the Pelotas Basin it is possible to see a thick sedimentary layer centered at $48°$W and $32°$S with up to 7 km of sediments. In the southern continental margin of Uruguay there is also a 7 km wedge of sediment and a thick sedimentary layer in the Rio Grande Cone is also observed.

An algorithm developed by Shiraiwa (1994) was used to estimate the gravitational effect due to the flexure of the lithosphere caused by the sedimentary loading. In this algorithm, the lithosphere is approximated by a thin elastic plate, with a load on its top (Timoshenko & Goodier, 1970). The gravitational effect of the deformed crust-mantle boundary is calculated by Parkers method (Parker, 1972). The parameters used to calculate gravitational effect of this deformation are: effective elastic thickness $= 10$ km; sediment density $= 2.4$ g/cm^3; crust oceanic rocks density $= 2.9$ g/cm^3; and mantle density $= 3.3$ g/cm^3. Figure 4 shows that the gravitational effect due to flexure is less than 10^{-1} mGal, therefore lower than the error in the free-air anomaly estimate.

Regional-Residual Separation

A deep source anomaly associated with variations in crust-mantle boundary and lower crust is observed and it should be removed in order to invert the anomalies associated with shallow sources.

For this purpose, a first degree polynomial surface was fitted to the original gravity data (Fig. 5) in order to estimate the regional gravity field. Figures 6 and 7 show the regional and residual anomalies, respectively. Gravity profiles were extracted from the residual anomaly shown in Figure 7.

LINEAR INVERSION METHODOLOGY

The solution of gravity data inversion is neither unique nor stable. Therefore it is an ill-posed problem (Hadamard, 1902). A way to reduce the instability and to guarantee the uniqueness of the solution is to introduce a priori information about unknown parameters.

Basically, gravity inversion problems can be subdivided into two groups: linear and nonlinear problems. The first group con-

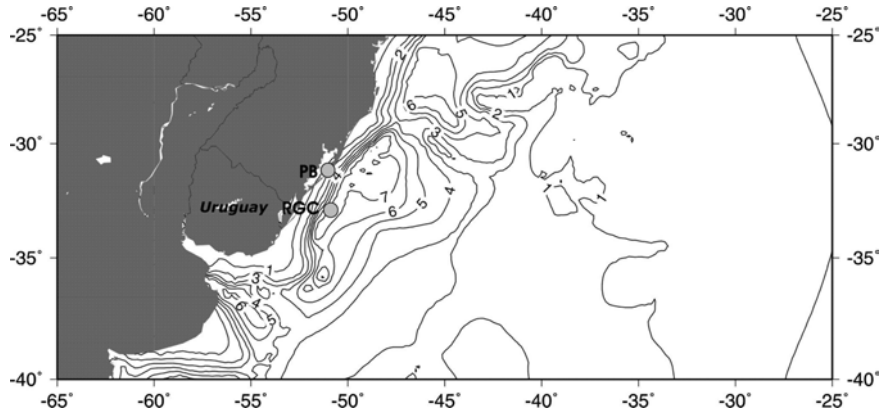

Figure 3 – (a) Sediment isopach map from Emery & Uchupy (1984). Contour interval = 1 km.

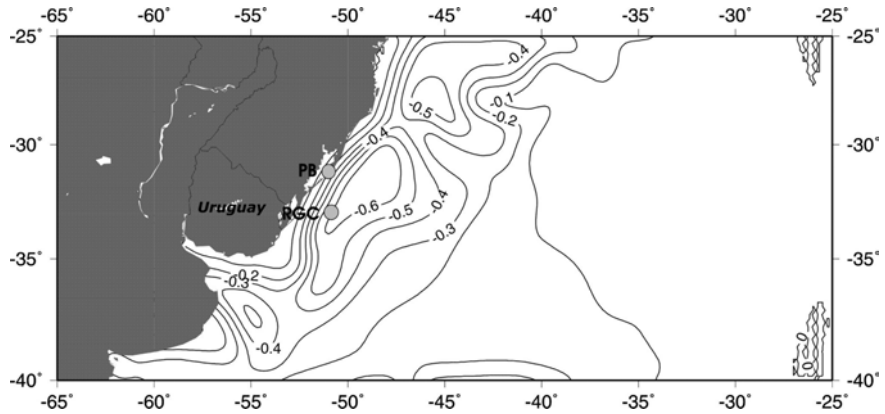

Figure 4 – Gravitational effect of crust-mantle boundary flexure due to sediment load on the Free-Air anomaly. Contour interval = 0.1 mGal.

tains several methods to calculate physical properties, which generally is density, while body geometry is fixed. These methods are used to map lateral and subsurface density distribution (e.g. Braile et al., 1974; Bear et al., 1995). Nonlinear methods are used to calculate body geometry while physical properties are fixed and these methods are useful to calculate anomalous bodys position and orientation and layers depths (e.g., Richardson & MacInnes, 1989; Barbosa et al., 1997).

We have chosen the linear inversion because, more than the geometry of the anomalous body, we wanted to learn about the stratigraphy of the basin and how it was formed. This information should be reflected in the density distribution.

The inverse problem can be expressed as a linear system like

$$\Delta g = G\Delta\rho\,, \tag{1}$$

where G is a linear operator (usually called sensitivity matrix) that describes the relationship between unknown model parameters $(\Delta\rho)$ and data (Δg). Matrix G will be defined using a forward method like that described in Talwani et al. (1959). To estimate $\Delta\rho$ we assume that a set of M juxtaposed cells represents the medium beneath the N points where the data Δg was collected.

Let us define $\Delta\rho$ as the M-dimensional density contrast vector to be estimated, and Δg as the N-dimensional gravity anomaly vector produced by the M cells. We can impose the fitting of gravity data by minimizing the functional

$$\varphi_{\Delta g}\,(\Delta g^0\,,\,\Delta g)\;=\;||\Delta g^0 - \Delta g||^2\,, \tag{2}$$

where $||\cdot||$ is the Euclidean norm. Estimating $\Delta\rho$ from Δg is a linear problem in this case. We will describe a method to estimate $\Delta\rho$ incorporating additional constraints.

Minimizing the functional below incorporates the relative equality constraints, namely the smooth density variation constraints

$$\varphi_x(\Delta\rho)\;=\;f_r\,||R\Delta\rho||^2\,, \tag{3}$$

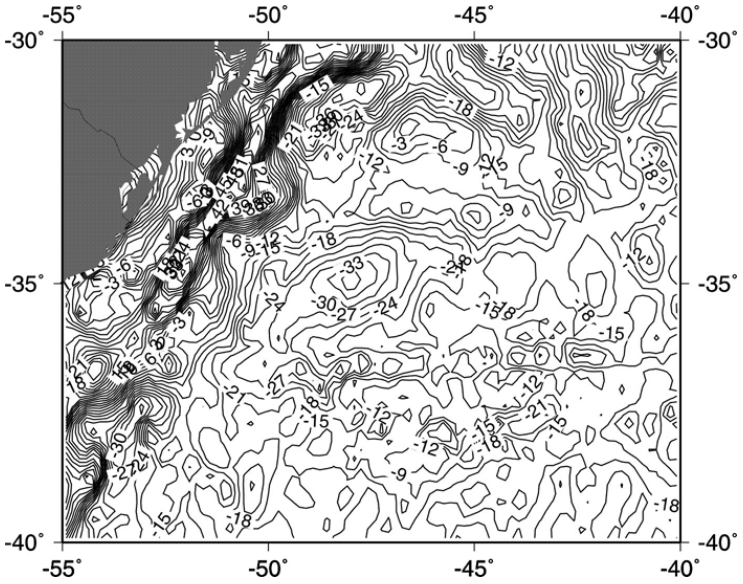

Figure 5 – Free-air anomaly. Contour interval = 0.3 mGal.

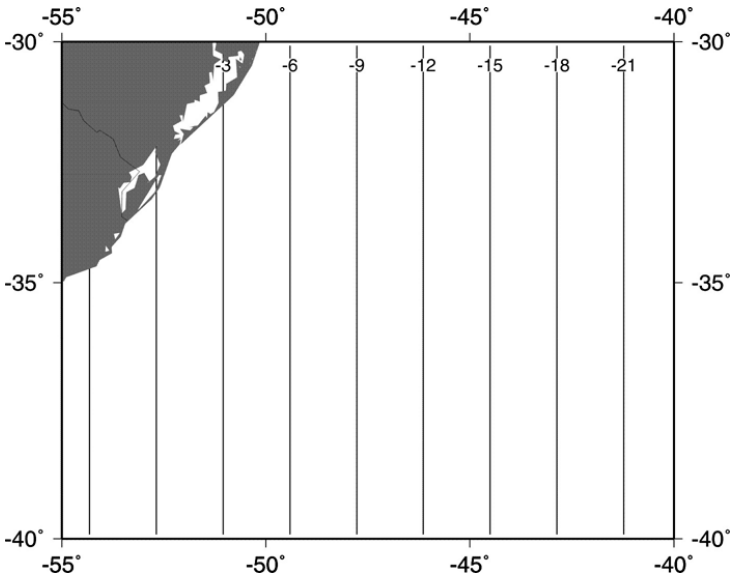

Figure 6 – Regional free-air anomaly (first-order polynomial surface). Contour interval = 0.3 mGal.

where f_r is a normalizing factor, R is a matrix $L \times M$, where L is the number of *a priori* relationships between pairs of parameters. if we know that the density of the *ith* block is twice the density of the *jth* block, then the *ith* and *jth* elements of the specific row of R that corresponds to the constraint will take values 1 and 2, respectively, whereas the rest of the elements in this row will be zero, giving rise to the expression $\Delta\rho_i - 2\Delta\rho_j \cong 0$ (Barbosa et al., 1997). Notice that it is possible to use different relationships in the same R matrix. For example, it can establish a linear relationship among the parameters forcing the increase of densities with depth.

Minimizing the functional below incorporates the absolute equality constraints

$$\varphi_a(\Delta\rho) = f_a \, ||A\Delta\rho - h||^2 , \qquad (4)$$

where A is an $H \times M$ matrix ($H \leq M$) whose rows contain only one non-null element, equal to unity (Barbosa et al., 1997), and h is an *a priori* specified H-dimensional vector for the den-

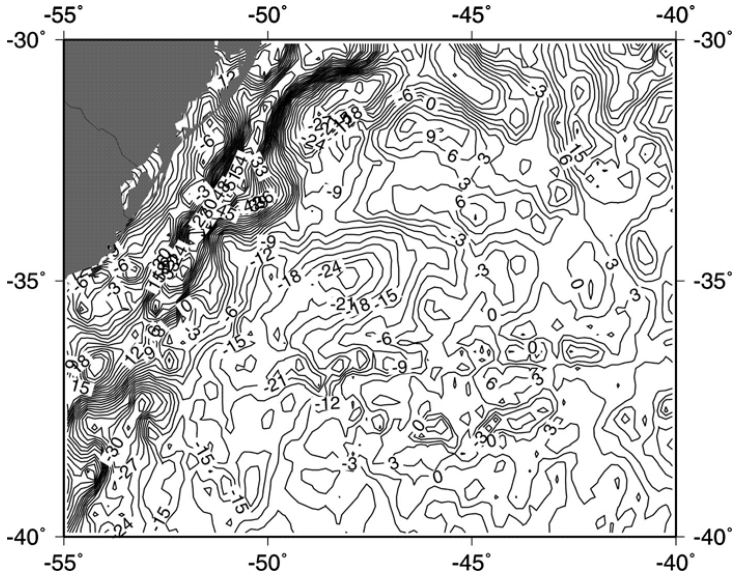

Figure 7 – Residual free-air anomaly. Contour interval = 0.3 mGal.

sities. The term f_a is a normalizing factor. For instance, if the *ith* parameter is known and its value is 0.5, we just have to set 1.0 in the *ith* column and first row of the matrix A, whereas the rest of the elements are set to zero. Accordingly, the first element of h will be 0.5.

The terms f_a and f_r are given by

$$f_a = \frac{||G||}{||A||} \quad \text{and} \quad f_r = \frac{||G||}{||R||} \tag{5}$$

where $||\cdot||$ is the Euclidean norm.

Incorporating the constraints (3) and (4) to the problem can be done by minimizing the unconstrained functional in the least-squares sense

$$\varphi(\Delta\rho) = \mu_r\varphi_r(\Delta\rho) + \mu_a\varphi_a(\Delta\rho) + \varphi_g(\Delta g^0, \Delta g). \tag{6}$$

Its solution to the vector $\Delta\rho$ is

$$\Delta\rho \left(\mu_a f_a(A^t A) + G^t G + \mu_r f_r(R^t R)\right)^{-1} \left(\mu_a f_a A^t h + G^t \Delta g^0\right). \tag{7}$$

The constants μ_a and μ_r are weights associated to each kind of constraints.

RESULTS OF DATA INVERSION

The proposed inversion methodology was applied to three gravity profiles shown in Figure 8: A-A, B-B and C-C. These profiles were extracted from the free-air anomaly residual map (Fig. 7). For each profile, the interpretative subsurface model consisted of 225 cells (15×15 cells with dimensions equal to 21 km and 0.35 km along x- and z- directions, respectively).

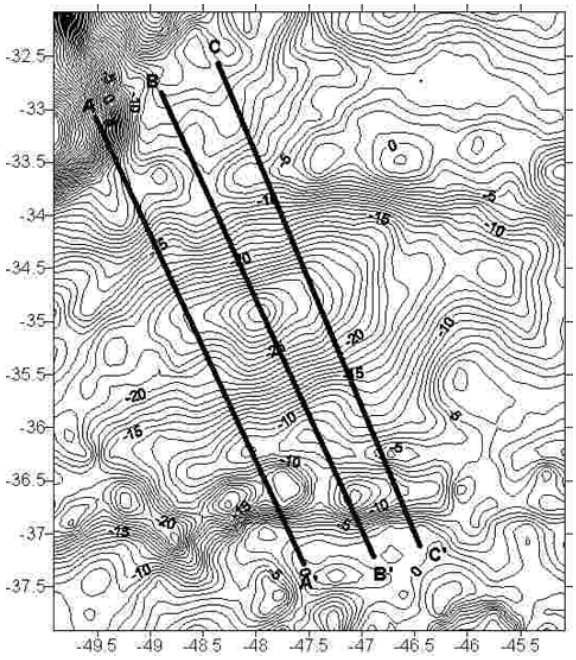

Figure 8 – Residual free-air anomaly and profiles used in the inversion procedure. Contour interval = 3 mGal.

Absolute constraints were set as follows: the densities of the two top layers, at depths between 4.8 km and 5.5 km, were fixed with values of 2.4 g/cm^3 based on seismic results given by Leyden et al. (1971). A background density of 3.0 g/cm^3 was

considered to represent the mean density of the crustal basement in the study area. Therefore, 0.6 g/cm^3 was the density contrast value set into the h vector of Equation 7. The two bottom layers, at depths between 9.2 km and 10 km, had cells fixed with values of 2.9 g/cm^3, which gives a density contrast of 0.1 g/cm^3. Cells constrained with absolute values are shown in Figure 9 as gray cells. Absolute constraints also helps in order to limit the range of possible values associated with the free-cells, thus biasing the solution towards a set of geologically sound density values. The weight associated with the absolute constraints was set equal to $\mu_a = 1.0$.

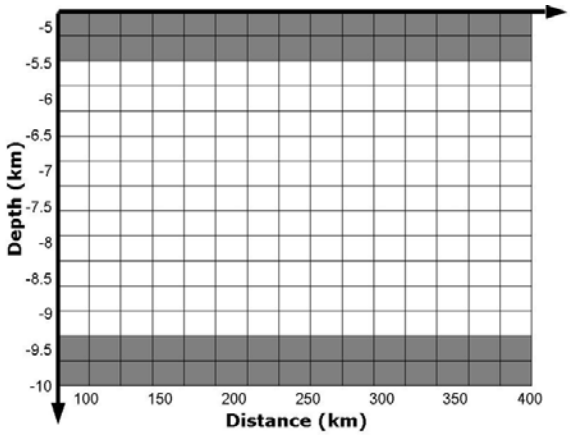

Figure 9 – Interpretative model used in the inversion procedures. The subsurface was subdivided into 225 cells (15×15). Absolute constraints were applied to gray cells in the two top layers by setting a density value of 2.4 g/cm^3 and in the two bottom layers by setting a density value of 2.9 g/cm^3.

Relative constraints were used in order to impose an overall smoothness on the density distribution estimate, as described in the methodology section. The weight associated with the relative constraints was set equal to $\mu_r = 0.1$. The combination of these two constraints provides a density distribution that is smooth and increases with depth, as was expected given the shapes of the anomalies together with the geological knowledge of the area.

Figures 10, 11 and 12 show the inversion results of the free-air anomalies profiles, A-A', B-B' and C-C', respectively. These results are consistent with a basin formation of evolution due to rifting and rapid initial subsidence. A uniform density distribution as shown in Figure 13, layer A, is expected if the first phase of sedimentation layer B refers to sedimentation well after rifting and oceanic lithosphere subsidence.

DISCUSSION

Sediment volume stored in this basin corresponds to approximately 50% of after-Miocene sediment volume stored in the Rio Grande Cone where gas-hydrates were found (Fontana, 1992).

LEPLAC seismic data are not available but Russo (1999) calculated an isopach map for the study area and its surroundings. This map shows a sedimentary thickness of 2.5 to 3 km, which is approximately equal to the inversion results, although there is no evidence in this map for the existence of a basin associated with the sedimentary layer.

Figure 14 shows the free-air anomaly overlapped by the tectonic map. We can see that the north limit of the negative free-air anomaly coincides with the Chuí Lineament, which extends to the Mid-Ocean Atlantic Ridge. The south limit of the anomaly appears to be another lineament and it is shown on the same figure, between the parallels $-37°$ and $-36.5°$. This lineament may represent an extension of the Meteor Fracture Zone.

The graben-like structure of this basin may be associated with a rifting event that occurred in response to adjacent continental margin uplifting (Leite, 2000) in the Eocene. This process was responsible firstly to open the graben and secondly to store the sediment, due to erosion post-uplifting.

The results of inversion, synthesized in Figure 13, also suggests a rapid subsidence in the rifting phase resulting in a uniform sediment storing as we can see in layer A. Post-rifting sediment storing, represented by layer B, occurred in the after-Miocene as a slower process, which results in thinner sediment layers with density lower than that found in layer A.

CONCLUSIONS

We performed a regional-residual separation on an integrated gravity map, through a first-order polynomial fitting, after which we extracted three free-air anomaly profiles across the main axis of a negative 23 mGal amplitude anomaly from the residual map. This anomaly is centered at $48°$W and $35°$S on the South Atlantic Ocean. We then estimated density distributions using a constrained linear gravity inversion methodology.

Inversion results suggest that the thickness in the deepest part of the basin is at least 3.0 km where the ocean bathymetry is 4,800 m. At this bathymetric depth we would expect to find oceanic crust.

We proposed a mechanism to a graben formation in SE Rio Grande Cone, based on an integrated interpretation of the inversion results added to geological and other geophysical constraints at the adjacent continental margin. It is important to notice that the anomaly appears to be situated between two lineaments where crustal shearing may have taken place, thus generating a possible stress mechanism that was responsible for the formation of this sedimentary basin.

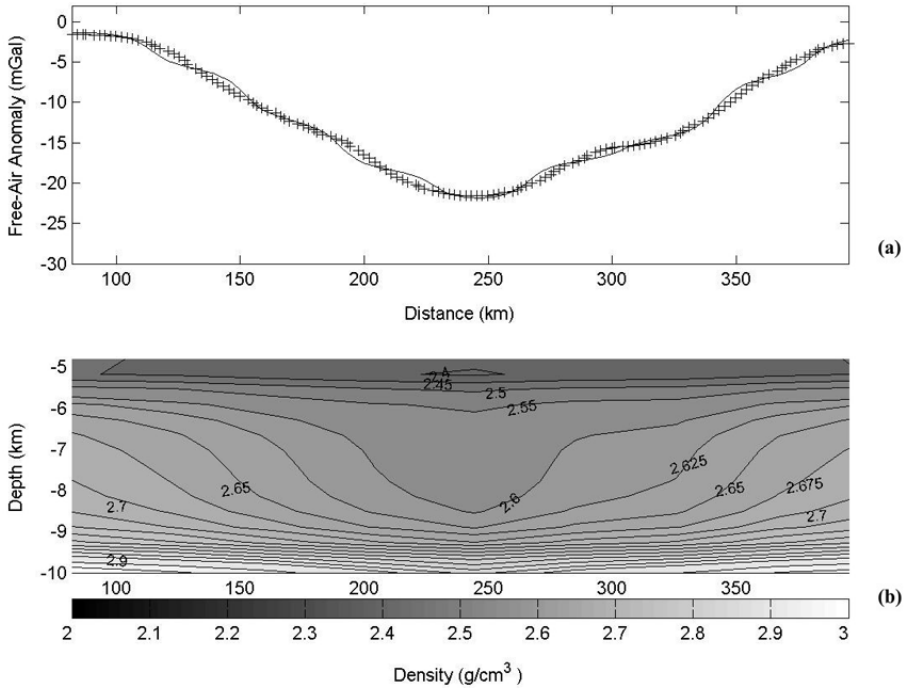

Figure 10 – Profile A-A: Two-dimensional density distribution estimate. (a) Observed (crosses) and fitted (solid line) residual free-air anomalies. (b) Estimated density distribution. Contour interval is 0.025 g/cm^3.

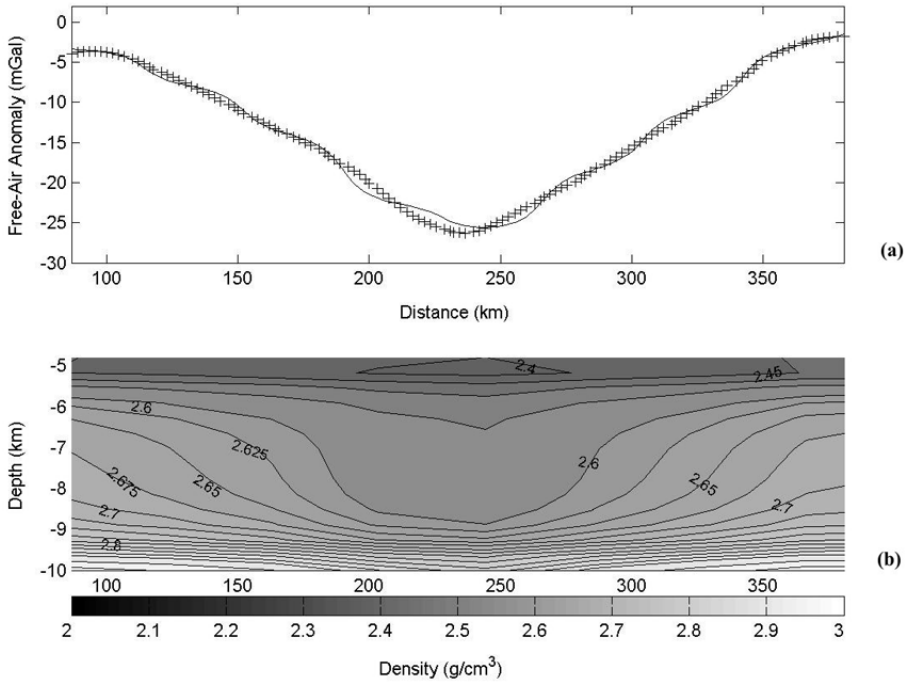

Figure 11 – Profile B-B: Two-dimensional density distribution estimate. (a) Observed (crosses) and fitted (solid line) residual free-air anomalies. (b) Estimated density distribution. Contour interval is 0.025 g/cm^3.

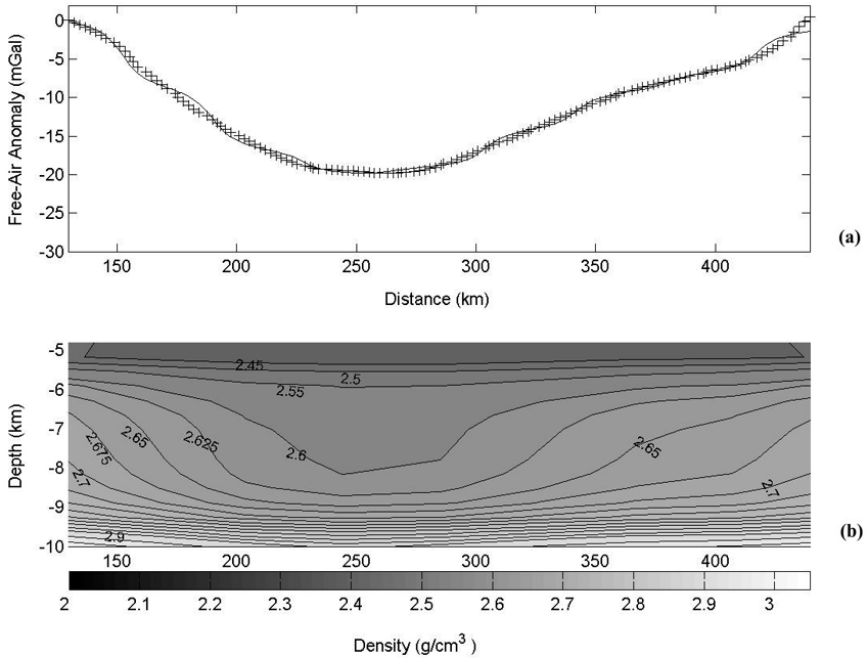

Figure 12 – Profile C-C: Two-dimensional density distribution estimate. (a) Observed (crosses) and fitted (solid line) residual free-air anomalies. (b) Estimated density distribution. Contour interval is 0.025 g/cm^3.

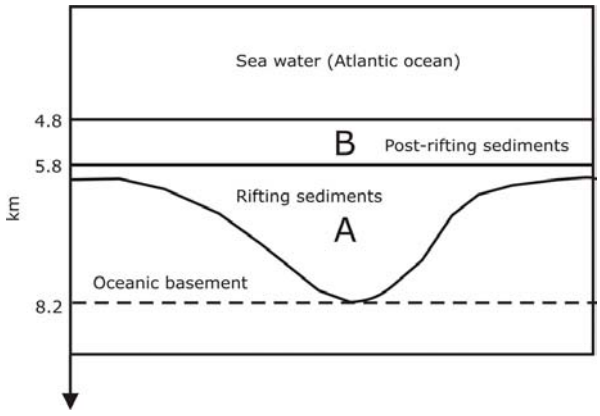

Figure 13 – Schematic layered model inferred from inversion results. Depth and horizontal distances are not at the same scale.

ACKNOWLEDGMENTS

We thank FAPESP for the financial support (Process number: 98/00107-8). The first author is specially thankful to the Institute of Astronomy, Geophysics and Atmospheric Sciences of the University of São Paulo, for all the computational, material and personal support during the time this work was carried out. We also thank Valéria Cristina F. Barbosa for her valuable comments, corrections and suggestions.

REFERÊNCIAS

ANDERSEN OB & KNUDSEN P. 1995. Global altimetric gravity map from the ERS-1 geodetic mission (cycle 1). Earth Observation Quarterly, 47: 1–5.

BARBOSA VCF, MEDEIROS WE & SILVA JB. 1997. Gravity inversion of basement relief using approximate equality constraints on depths. Geophysics, 62: 1745–1757.

BARBOSA VCF, SILVA JBC & MEDEIROS WE. 2002. Practical applications of uniqueness theorem in gravimetry: Part II – Pragmatic incorpora-

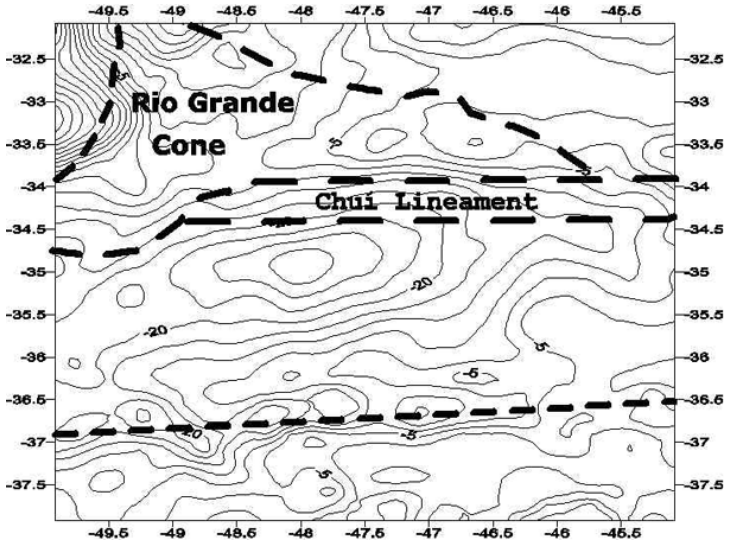

Figure 14 – Free-air anomaly map overlapped by tectonic structures over the study area. The E-W dotted line situated between the parallels $-37°$ and $-36.5°$ indicates a possible lineament.

tion of concrete geologic information. Geophysics, 67: 795–800.

BEAR GW, AL-SHUKRI HJ & RUDMAN AJ. 1995. Linear inversion of gravity data for 3-D density distributions. Geophysics, 60: 1354–1364.

BRAILE LW, KELLER GR & PEEPLES WJ. 1974. Inversions of gravity data for two-dimensional density distributions. J. Geophys. Res., 19: 2017–2021.

EMERY KO & UCHUPI E. 1984. The Geology of the Atlantic Ocean, Springer-Verlag, New York, 1050pp.

FONTANA RL. 1992. Investigações Geofísicas Preliminares Sobre o Cone do Rio Grande e Bacia de Pelotas – Brasil. Acta Geol. Leop., 13(30): 161–170.

HADAMARD J. 1902. Sur les problèmes aux dérivées et leur signification physique: Bull Princeton Univ., 13: 1–20.

LEITE EP, MOLINA EC & USSAMI N. 1999. Integração de dados de gravimetria marinha e de altimetria por satélite (GEOSAT/ERM) no Atlântico Sul ($25/40°$S e $65/25°$W). Rev. Bras. Geofísica, 17: 145–161.

LEITE EP. 2000. Estrutura da litosfera a partir da interpretação de dados geopotenciais na região compreendida entre $25/40°$S e $25/60°$W. Dissertação de Mestrado. IAG/USP, São Paulo, 109 pp.

LEYDEN R, LUDWING WJ & EWING M. 1971. Structure of the continental margin off Punta del Este, Uruguay, and Rio de Janeiro, Brazil. Am. Ass. Petrol. Geol., Bull. 55(12): 2161–2173.

PARKER RL. 1972. The rapid calculation of potential anomalies. Geophys. J. Roy Astr. Soc., 31: 447–455.

RICHARDSON RM & MACINNES SC. 1989. The inversion of gravity data into three-dimensional polyhedral models. J. Geophys. Res., 94: 7555–7562.

RUSSO LR. 1999. LEPLAC: Isópacas de sedimentos e profundidade do embasamento na margem continental brasileira. $6°$ Congresso Internacional da Sociedade Brasileira de Geofísica. Resumo expandido (CD-ROM).

SHIRAIWA S. 1994. Flexura da litosfera continental sob os Andes Centrais e a origem da Bacia do Pantanal, Tese de Doutoramento, Univ. de São Paulo, São Paulo, Brasil, 110 pp.

SILVA JBC, MEDEIROS WE & BARBOSA VCF. 2002. Practical applications of uniqueness theorems in gravimetry: Part I – Constructing sound interpretation methods. Geophysics, 67: 788–794.

TALWANI M, LAMAR WORZEL J & LANDISMAN M. 1959. Rapid Gravity Computations for two-dimensional bodies with application to the Mendocino Submarine Fracture Zone. J. Geophys. Res., 64(1): 49–59.

TIMOSHENKO S & GOODIER JN. 1970. Theory of Elasticity. McGraw-Hill, New York, 567 pp.

NOTES ABOUT THE AUTHORS

Emilson Pereira Leite. Collaborator Researcher at the DGRN/IG-Unicamp. He received his Master's (2000) and Ph.D. (2005) degrees in Geophysics both from IAG/USP. His current research interests are in the area of spatial modeling and integration of geophysical and remotely sensed data and inversion methods in Geophysics.

Naomi Ussami. Associated Professor at the IAG/USP. She received her Ph.D. degree in Geophysics from Durham University, England (1986) and she did her post-doctorate at Cornell University (1995). Her current areas of research are Tectonophysics and Potential Methods in Geophysics.